MOLECULAR AND CELLULAR BIOLOGY, Dec. 2004, p. 10933–10940 Vol. 24, No. 24
0270-7306/04/$08.00+0 DOI: 10.1128/MCB.24.24.10933–10940.2004

The Mitochondrial *SDHD* Gene Is Required for Early Embryogenesis, and Its Partial Deficiency Results in Persistent Carotid Body Glomus Cell Activation with Full Responsiveness to Hypoxia

José I. Piruat,[1] C. Oscar Pintado,[2] Patricia Ortega-Sáenz,[1] Marta Roche,[1] and José López-Barneo[1]*

Laboratorio de Investigaciones Biomédicas, Hospital Universitario Virgen del Rocío,[1] and Centro de Producción y Experimentación Animal, Universidad de Sevilla,[2] Seville, Spain

Received 19 July 2004/Returned for modification 3 September 2004/Accepted 23 September 2004

The *SDHD* gene encodes one of the two membrane-anchoring proteins of the succinate dehydrogenase (complex II) of the mitochondrial electron transport chain. This gene has recently been proposed to be involved in oxygen sensing because mutations that cause loss of its function produce hereditary familiar paraganglioma, a tumor of the carotid body (CB), the main arterial chemoreceptor that senses oxygen levels in the blood. Here, we report the generation of a *SDHD* knockout mouse, which to our knowledge is the first mammalian model lacking a protein of the electron transport chain. Homozygous $SDHD^{-/-}$ animals die at early embryonic stages. Heterozygous $SDHD^{+/-}$ mice show a general, noncompensated deficiency of succinate dehydrogenase activity without alterations in body weight or major physiological dysfunction. The responsiveness to hypoxia of CBs from $SDHD^{+/-}$ mice remains intact, although the loss of an *SDHD* allele results in abnormal enhancement of resting CB activity due to a decrease of K^+ conductance and persistent Ca^{2+} influx into glomus cells. This CB overactivity is linked to a subtle glomus cell hypertrophy and hyperplasia. These observations indicate that constitutive activation of $SDHD^{+/-}$ glomus cells precedes CB tumor transformation. They also suggest that, contrary to previous beliefs, mitochondrial complex II is not directly involved in CB oxygen sensing.

Mitochondrial complex II (succinate dehydrogenase [SDH]) plays major biological roles in the Krebs cycle and the mitochondrial electron transport chain, oxidizing succinate to fumarate and transferring electrons to the ubiquinone pool (9, 12). SDH has also been proposed to have an antioxidant function, protecting against superoxide production in mitochondria, and to participate in oxygen (O_2) sensing (3, 7, 22, 27). Deficiencies of any of the four subunits of SDH (A, B, C, and D) are associated with a broad spectrum of human diseases, ranging from myo- and encephalopathies to aging and tumor formation. Mutations in SDHA, the matrix-faced flavoprotein, result in dysfunction of the energy metabolism, e.g., Leigh syndrome or exercise intolerance, whereas mutations either in the iron-sulfur protein SDHB or in SDHC and SDHD, the membrane-anchoring proteins that contain one heme and are essential for ubiquinone binding, are more often associated with pheochromocytoma and paraganglioma (1, 22, 23). Specifically, mutations in *SDHD* are the main cause of familiar hereditary paraganglioma (PGL) (3) a mostly benign, highly vascularized tumor of the carotid body (CB). *SDHD* is the first tumor suppressor gene identified which encodes a mitochondrial protein.

The CB is the main arterial chemoreceptor that senses blood O_2 concentration. It is a highly irrigated bilateral organ, located at the bifurcation of the carotid artery and derived from the neural crest. Upon exposure to acute hypoxia, neurosecretory CB glomus cells release transmitters which activate afferent sensory fibers connected with brain stem centers to elicit hyperventilation and sympathetic activation (see references 14 and 15 for reviews). Similar to CBs of individuals exposed chronically to hypoxia (11, 25), PGL tumors display cellular hyperplasia or anaplasia in the absence of hypoxic stimulus (3). Moreover, the prevalence of paragangliomas in individuals with *SDHD* mutations increases in populations living at high altitudes (2). Thus, it has been proposed that SDHD participates in O_2 sensing and that PGL tumors are induced by defects in the detection of blood O_2 levels (3, 4, 7, 22).

Advance in the study of SDH function is, however, hampered by the lack of mammalian genetic models of SDH deficiency. To determine the possible involvement of the mitochondrial complex II in O_2 sensing and the pathophysiology of hereditary CB PGL, we have generated a knockout mouse carrying a null allele of the *SDHD* gene. Here we describe the major general effects of *SDHD* deficiency and the physiological features of CB glomus cells from *SDHD* knockout mice.

MATERIALS AND METHODS

Generation of $SDHD^{+/-}$ knockout mice. A cDNA homolog to the human succinate dehydrogenase D gene (accession number BF161694) was used as a probe for the screening of a lambda FIXII vector-based genomic library of mouse strain 129SvJ by hybridization of phage-infected bacterial plaques. Isolated genomic DNA was used for making a targeting construct consisting of a *neo* cassette that replaced exons 2, 3, and 4 of the *SDHD* gene, flanked by two arms of homolog DNA (4.0 and 4.4 kb, respectively) that allow for homologous recombination. The targeting construct was electroporated into mouse embryonic stem (ES) cells. Clones resistant to 0.2 mg of Geneticin G418 per ml were selected and analyzed for proper targeting at the *SDHD* locus. Male chimeras were generated and mated with 129SvJ wild-type females, which gave F_1 offspring with heterozygous $SDHD^{+/-}$ individuals. Animal care and experimentation were according to the institutional animal care committee guidelines.

* Corresponding author. Mailing address: Laboratorio de Investigaciones Biomédicas, Edificio de Laboratorios, 2ª Planta, Hospital Universitario Virgen del Rocío, Avenida Manuel Siurot s/n, E-41013, Seville, Spain. Phone: (34)-954-617090 or (34)-955-012648. Fax: (34)-954-617301. E-mail: jose.l.barneo.sspa@juntadeandalucia.es.

Nucleic acid analysis. Total DNA from ES cells, toe tips, and embryos was prepared by incubation in 20 mM Tris-HCl (pH 8.5)–5 mM EDTA–1% sodium dodecyl sulfate–400 mM NaCl–0.1 mg of proteinase K per ml at 57°C for 2 h. For Southern blotting, 20 μg of genomic DNA was digested and loaded onto a Tris-acetate-EDTA–agarose gel. For tissue RNA analysis, organs were dissected and homogenized in TRIzol reagent according to the manufacturer's instructions. For Northern blotting, 10 to 15 μg of RNA per sample was loaded onto a formaldehyde-agarose gel. Electrophoresis and transfer of nucleic acids to Hybond-N nylon membranes were performed by standard methods. Hybridization was done at 42°C in Ultra-Hyb hybridization buffer. Gel-purified DNA probes were radiolabeled with [α-^{32}P]dCTP by using the Rediprime kit.

Embryo analysis. To obtain *SDHD*$^{-/-}$ embryos, heterozygous *SDHD*$^{+/-}$ parents were mated. Females were sacrificed at different days after copula took place for dissection of the uterus, after which maternal tissue was carefully removed, and embryos were dissected for DNA analysis. In order to discriminate between the wild-type and the mutant allele a three-primer approach was designed. Primers 5′-TCAGTGACAACGTCGAGCAC-3′, 5′-CAAGGTCGGAA CCCAGAGAT-3′, and 5′-ATAGCCAGCCAGGTAGTTCC-3′ give products of 1.8 kb for the wild type and 1.25 kb for the mutant *SDHD* allele.

Isolation of mitochondria. Isolation of mitochondria from mouse tissues was performed as reported previously (6). Tissues were dissected and washed in ice-cold phosphate-buffered saline. The entire process of mitochondrion isolation was carried out at 4°C, with samples kept on ice. Organs were cut with scissors in small fragments in 2 ml of homogenization medium (320 mM sucrose–1 mM EDTA–10 mM Tris-HCl [pH 7.4] for liver and kidney and 75 mM sucrose–225 mM sorbitol–1 mM EGTA–0.1 fatty acid-free bovine serum albumin–10 mM Tris-HCl [pH 7.4] for brain and heart). Cells were broken with 10 to 15 strokes in a Dounce homogenizer with a motor-driven pestle. The homogenate was centrifuged at 4,000 rpm for 6 min in a microcentrifuge, and mitochondrion-containing supernatant was collected. Mitochondria were spun down by centrifugation for 10 min at 13,000 rpm, washed twice with medium B (250 mM sucrose, 2 mM HEPES, 0.1 mM EGTA), and resuspended in a final volume of about 250 μl of medium B. The mitochondrion suspension was aliquoted (40 μl), flash frozen in liquid nitrogen, and kept at −80°C until used. The protein concentration was determined according to Bradford's method, with samples diluted in 0.05% sodium dodecyl sulfate.

Measurement of activities of mitochondrial complexes. Activities of mitochondrial complexes were determined in a Beckman DU-640 spectrophotometer, as described by Birch-Machin and Turnbull (5) with slight modifications. All reagents were purchased from Sigma unless otherwise indicated. For mitochondrial complex I and II activities, 30 to 50 μg of protein was assayed at 30°C. Samples were diluted 1:4 in the assay reaction buffer (25 mM KH_2PO_4 [pH 7.2], 5 mM $MgCl_2$, 3 mM potassium cyanide, 2.5 mg of bovine serum albumin per ml) and freeze-thawed three times with liquid nitrogen before the assay. For mitochondrial complex I activity, the rotenone-sensitive NADH dehydrogenase activity was measured as the decrease in absorbance at 340 nm, referred to 425 nm, due to oxidation of 130 μM NADH (Roche) in presence of 3.6 μM antimycin and 130 μM ubiquinone-1. Absorbance was measured for 2 min before and after addition of 5 μM rotenone to the reaction mixture. During this period the rate of decrease of absorbance was linear. Differences between rates were considered for determining activity due to mitochondrial complex I. To evaluate the mitochondrial complex II activity, succinate dehydrogenase activity was measured for a period of 2 min as the decrease in the absorbance at 600 nm due to the reduction of 50 μM 2,6-dichlorophenol-indophenol (DCPIP) coupled to reduction of 130 μM ubiquinone-1. The reaction was carried out in presence of 3.6 μM antimycin, 5 μM rotenone, and 10 mM succinate.

Carotid body immunohistochemistry. Bifurcations containing carotid bodies were dissected and fixed in formalin (Sigma) at 4°C for 16 h. Tissues were dehydrated and paraffin embedded, and 10-μm slices were obtained by using an RM2125 microtome (Leica Microsystems). Immunohistochemistry was performed according to standard procedures. For detection of glomus cells, tissues were immunostained with a rabbit polyclonal antityrosine hydroxylase (PelFreez). After immunodetection with peroxidase-conjugated secondary antibody, tissue samples were counterstained with hematoxylin.

Amperometric recordings in carotid body slices. Mouse carotid body slicing and monitoring of single-cell secretion was done according to the same basic procedures described for rats (18, 20). Slices were continuously perfused with a solution containing 117 mM NaCl, 4.5 mM KCl, 23 mM $NaHCO_3$, 1 mM $MgCl_2$, 2.5 mM $CaCl_2$, 5 mM glucose, and 5 mM sucrose. The normoxic solution was bubbled with a gas mixture of 5% CO_2, 20% O_2, and 75% N_2 (O_2 tension of ~150 mm Hg). The hypoxic solution was bubbled with 5% CO_2 and 95% N_2 to reach an O_2 tension in the chamber of ~20 mm of Hg. All experiments were done at a chamber temperature of ~36°C. The cumulative secretion signal is the sum of the time integral of successive amperometric events. The secretion rate (in femtocoulombs per minute) was calculated as the amount of charge transferred to the recording electrode during a given time period.

Patch clamp recordings in dispersed CB glomus cells. Mouse carotid bodies were incubated for 20 min in an enzyme solution (1 ml of phosphate-buffered saline with 0.6 mg of collagenase II, 0.3 mg of trypsin, 40 μl of elastase I, 0.3 mg of bovine serum albumin, and 10 μl of $CaCl_2$ from a 5 mM stock solution) at 37°C, and the cells were mechanically dispersed by using fire-polished Pasteur pipettes. Cells were plated on slivers of glass coverslips treated with poly-L-lysine and kept in culture medium (Dulbecco's modified Eagle's medium with 10% fetal bovine serum, 1% antibiotics, 1% L-glutamine, and 84 μU of insulin per ml). Macroscopic ionic currents were recorded by using the whole-cell configuration of the patch clamp technique as adapted to our laboratory (20, 24). The standard extracellular solution contained 117 mM NaCl, 4.5 mM KCl, 23 mM $NaHCO_3$, 1 mM $MgCl_2$, 2.5 mM $CaCl_2$, 5 mM glucose, and 5 mM sucrose, and the pH was adjusted by bubbling with 5% CO_2. The standard internal solution (inside the pipette and the cell) contained 80 mM K-glutamate, 30 mM KCl, 20 mM KF, 1 mM EGTA, and 4 mM Mg-ATP (pH 7.3) adjusted with KOH. Cell capacity was estimated from the time integral of capacitative current transients recorded by application of 2-ms depolarizing pulses of 20 mV from the holding potential of −80 mV. To calculate cell size, we assumed a constant membrane-specific capacity of 1 μF/cm^2. Conductance-voltage curves were obtained from the normalized amplitude of inward K^+ tail currents recorded at the end of depolarizing pulses. For these experiments, we used an external solution with 30 mM KCl (NaCl was reduced to 87 mM to maintain constant the osmolality). All of the electrophysiological experiments were done at room temperature (~22°C).

Statistical analysis. Unless otherwise specified, data are expressed as means ± standard errors of the means, with the number of experiments (*n*) indicated. Statistical analysis was performed with the unpaired Student *t* test. A *P* value of <0.05 was considered statistically significant.

RESULTS

Generation of the *SDHD*$^{+/-}$ knockout mouse. In order to generate a mutant allele of the *SDHD* gene, we first performed a screening of a library of mouse genomic DNA, based on lambda phage, with a cDNA probe containing the entire *SDHD* coding sequence. Two fragments of approximately 16 and 19 kb were isolated. Restriction analysis and sequencing confirmed, by comparison with the Ensembl Genome Browser (www.ensembl.org), that they both contained the entire genomic DNA corresponding to the *SDHD* gene. These DNA fragments were used for making the targeting construct. The generation of the mutant *SDHD* allele is shown schematically in Fig. 1A. The targeting construct contained the prokaryotic neomycin resistance gene (*neo*) flanked by genomic DNA homologous to the *SDHD* locus. ES cells were electroporated with this targeting construct and selected for Geneticin resistance. ES cell clones were isolated and analyzed by Southern blotting for proper integration of the nonfunctional allele (Fig. 1B). Homologous recombination replaced the wild-type allele by the mutant allele lacking exons 2, 3, and 4. The selected clones were used for blastocyst injection to generate chimeras from which we obtained heterozygous F_1 offspring, which were also identified by Southern blotting (Fig. 1C).

Embryo lethality of *SDHD*$^{-/-}$ mice. To date, we have genotyped 152 animals born from mating between heterozygous parents, of which 50 (33%) were *SDHD*$^{+/+}$ and 102 (66%) were *SDHD*$^{+/-}$, with no *SDHD*$^{-/-}$ animals detected. These are the relative frequencies expected for a Mendelian-type inheritance with lethality for homozygous mutant embryos. The analysis of embryos from heterozygous pregnant females mated with heterozygous males indicates that *SDHD*$^{-/-}$ animals die at early stages of organogenesis. Figure 2 shows that at 7.5 days postconception (dpc) all developing embryos from

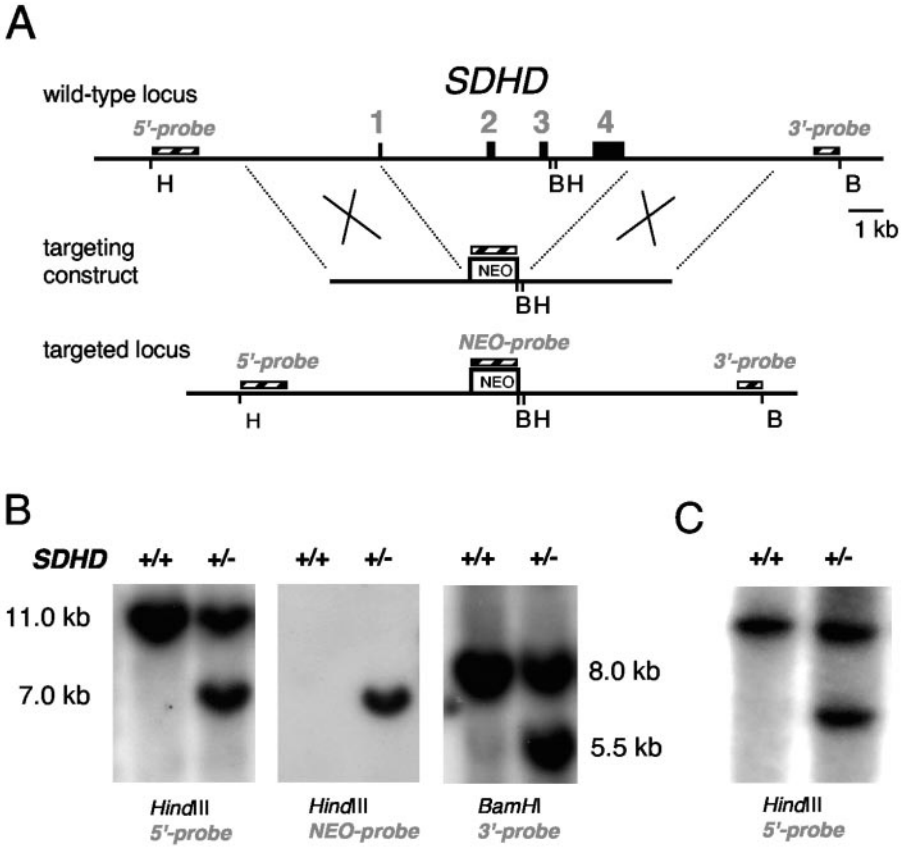

FIG. 1. (A) Generation of a null allele of the *SDHD* gene. Gene targeting replaced the wild-type allele by a nonfunctional allele lacking exons 2, 3, and 4. The two homologous fragments of genomic DNA (4.0 and 4.4 kb) flanking the prokaryotic neomycin resistance (*neo*) gene allow for homologous recombination. B, BamHI; H, HindIII. (B) Selected ES cell clones were analyzed for correct gene targeting at the *SDHD* locus by Southern blotting. Digested DNA was hybridized with the indicated probes, giving additional bands of the indicated sizes in the heterozygous (+/−) ES clone with respect to the homozygous wild type (+/+). (C). Southern blot genotyping of *SDHD* knockout mice.

a mating had the same appearance (Fig. 2A), whereas at 9.5 dpc approximately one-fourth of embryos were stalled at a previous stage (Fig. 2B). To further analyze the embryonic development of these mice, we dissected the embryos from the maternal decidua at 7.5 dpc, among which some were clearly arrested several hours before (Fig. 2C and D). The dissected embryos were analyzed by PCR (Fig. 2E). The use of specific primers for both the wild-type and mutant alleles showed that those embryos with normal appearance (Fig. 2C) corresponded to either the wild-type ($SDHD^{+/+}$; one 1.8-kb band) or the heterozygous ($SDHD^{+/-}$; two bands of 1.8 and 1.25 kb) mice, whereas the stalled embryos (Fig. 2D) corresponded to the homozygous $SDHD^{-/-}$ (1.25-kb band) mice. These observations indicate that $SDHD^{-/-}$ mutants die before 7.5 dpc in the embryo development, coinciding with the early stage of organogenesis.

Functional analysis of the *SDHD* gene in heterozygous animals. We analyzed the effect of the removal of one copy of the *SDHD* gene on both the expression of the remaining allele and the activity of mitochondrial complex II. In $SDHD^{+/-}$ animals a general decrease of the steady-state level of the SDHD mRNA was observed in heart, brain, kidney, and liver (Fig. 3A). Consistently, in mitochondria isolated from the same tissues, succinate dehydrogenase activity was ~50% lower than normal, whereas mitochondrial complex I activity remained unchanged (Fig. 3B). Hence, the deficit of mitochondrial complex II activity correlates with the absence of one of the functional alleles of the *SDHD* gene, indicating that a compensatory up-regulation of the remaining wild-type allele does not take place. Despite the general decrease of complex II activity, $SDHD^{+/-}$ animals did not show signs of gross physiologic alterations. At 6 months, the animal weight for males was 30.8 ± 0.7 g (n = 13) for $SDHD^{+/+}$ animals versus 31 ± 0.6 g (n = 22) for $SDHD^{+/-}$ animals; that for females was 23.4 ± 1.1 g (n = 11) for $SDHD^{+/+}$ animals versus 22.7 ± 0.5 g (n = 13) for $SDHD^{+/-}$ animals.

CB glomus cell secretory activity in response to hypoxia. The most frequent manifestation of SDHD deficiency in humans is the hereditary CB PGL (3, 4). PGL tumors display cellular hyperplasia and CB hypertrophy, similar to what occurs in individuals exposed to chronic hypoxia (11, 25). Therefore, it has been proposed that *SDHD* participates in O_2 sensing and that the ultimate cause of PGL tumors is a defect in sensing environmental O_2 levels (3, 4, 7, 22). We have tested in young adult mice whether a partial *SDHD* deficit and the reduction of mitochondrial complex II activity alter CB function by monitoring catecholamine secretion from single glomus cells in slices of the whole organ. Similar to the case for rat CB slices (18, 20), the response to hypoxia of glomus cells in mouse CB slices was characterized by a sharp and reversible burst of secretory events (Fig. 4A). This response was maintained, or

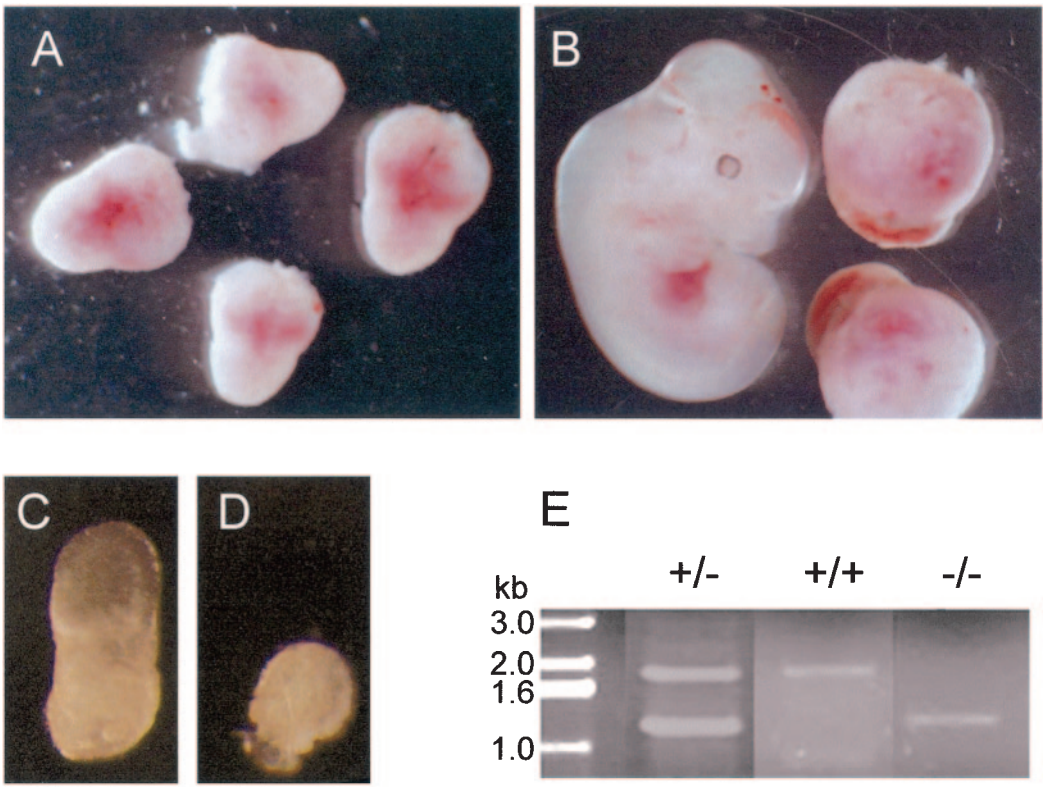

FIG. 2. (A and B) Embryos dissected at (A) 7.5 dpc and (B) 9.5 dpc from *SDHD*$^{+/-}$ females mated with *SDHD*$^{+/-}$ males. Note differences between embryos in panel B, which are not observable in panel A. (C and D) Embryos dissected from maternal decidua at 7.5 dpc. (E) PCR analysis of embryos dissected at 7.5 dpc. Stalled embryos show only the band corresponding to the mutant *SDHD* allele (−/−; 1.25 kb), whereas normal embryos show the pattern expected for either wild-type (+/+; 1.8 kb) or heterozygous (+/−; both bands) individuals.

even augmented, in *SDHD*$^{+/-}$ mice (Fig. 4B and C), indicating that a partial deficiency of complex II activity does not alter glomus cell responsiveness to hypoxia. However, spontaneous CB activity under normoxic conditions was increased by ~2.4-fold ($P < 0.05$) in *SDHD*$^{+/-}$ animals compared with wild-type littermates (Fig. 4D). The higher resting excitability of CB cells in *SDHD*$^{+/-}$ animals also explained the slight increase of the hypoxic response. The spontaneous secretory activity of *SDHD*$^{+/-}$ glomus cells was reversibly abolished by blockade of Ca^{2+} channels with Cd^{2+} (Fig. 4E), thus suggesting that it was due to persistent extracellular Ca^{2+} influx through membrane channels (18, 20, 24).

Electrophysiological and morphological characterization of CB glomus cells in *SDHD*$^{+/-}$ mice. To analyze in further detail the molecular changes underlying CB activation in *SDHD*$^{+/-}$ mice, we studied the K^+ currents in patch-clamped glomus cells, as it is known that in this preparation K^+ channels regulate membrane potential and cellular excitability (see reference 20 and references therein). Representative families of K^+ currents from *SDHD*$^{+/+}$ and *SDHD*$^{+/-}$ glomus cells are illustrated in Fig. 5A and B. The average K^+ current density- and conductance-voltage relationships are shown in Fig. 5C and D, respectively. In wild-type glomus cells the increase in K^+ current amplitude induced by membrane depolarization showed a characteristic saturation at positive membrane potentials (Fig. 5A and C). This reflects a K^+ current component mediated by voltage- and Ca^{2+}-activated K^+ channels whose probability of being open decreases at membrane voltages near the apparent Ca^{2+} equilibrium potential (16, 21). Interestingly, under the experimental conditions of our study, this current component almost disappeared in glomus cells from *SDHD*$^{+/-}$ mice (Fig. 5B). In *SDHD*$^{+/-}$ glomus cells, the K^+ current-voltage relationship was almost linear (Fig. 5C), and the total K^+ current density decreased (3.55 ± 0.63 pA/μm^2 [$n = 11$] for *SDHD*$^{+/+}$ mice and 2.96 ± 0.11 pA/μm^2 [$n = 8$] for *SDHD*$^{+/-}$ mice at +20 mV). In addition, close inspection of the macroscopic K^+ current recordings indicated that their activation threshold increased in *SDHD*$^{+/-}$ glomus cells (compare the current records obtained at −30, −20, and −10 mV in Fig. 5A and B). This was confirmed by the analysis of the K^+ conductance-voltage relationships, which demonstrated a ~10-mV displacement to positive membrane potentials of the activation threshold of K^+ channels in *SDHD*$^{+/-}$ glomus cells (Fig. 5D). Although a complete biophysical analysis of ion channels in *SDHD*$^{+/-}$ glomus cells is outside the scope of the present study, the data suggest that the sensitivity to Ca^{2+} of K^+ channels could be decreased in SDHD-deficient animals. It is known that Ca^{2+}-activated K^+ channels contribute to the resting potential of rodent glomus cells (20, 26) and that in most tissues these channels act as counterregulatory devices that prevent excessive cell depolarization. Therefore, the biophysical changes observed in patch-clamped *SDHD*$^{+/-}$ glomus cells could account for the persistent secretory activity detected by amperometry in CB slices.

The constitutive functional activation of CB glomus cells observed in SDHD-deficient mice occurred without obvious

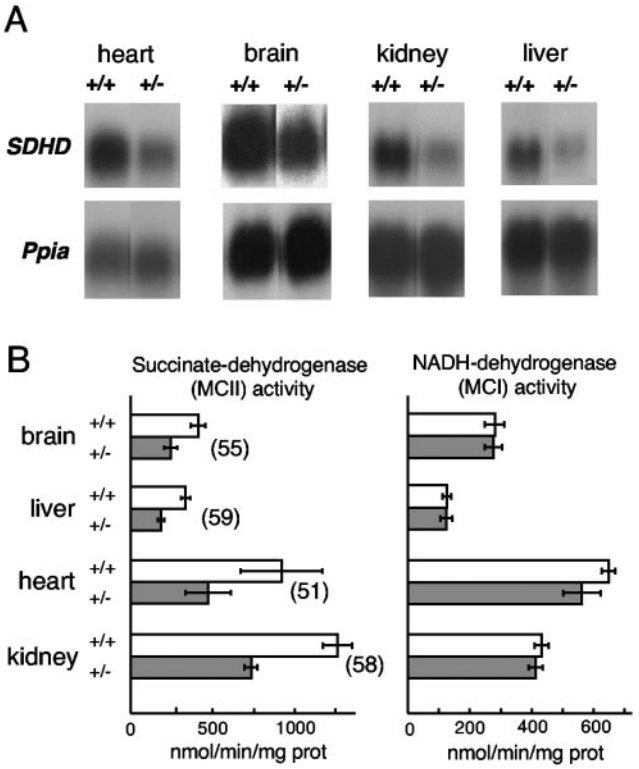

FIG. 3. (A) *SDHD* mRNA expression in the indicated tissues. Total RNA was hybridized with an *SDHD* cDNA-containing probe. The *Ppia* gene, encoding cyclophilin, was used as loading control. (B) Mitochondrial succinate-dehydrogenase (MCII) and NADH-dehydrogenase (MCI) activities in mouse tissues. Data are the averages from four animals per tissue and genotype. Error bars indicate the standard error. In all tissues MCII activities in $SDHD^{+/+}$ and $SDHD^{+/-}$ mice were significantly different ($P < 0.05$). Numbers in parentheses indicate the relative activity (in percent) in $SDHD^{+/-}$ with respect to $SDHD^{+/+}$ mice.

organ enlargement or gross histological modifications. However, the glomus cell membrane surface (estimated from the values of cell capacitance measured in patch-clamped cells) increased from 254 ± 57 μm^2 ($n = 25$) in wild-type to 297 ± 17 μm^2 ($n = 17$) in $SDHD^{+/-}$ glomus cells ($P < 0.05$). We have also observed a slight, although significant, increase in the percentage of glomus cells, identified by their immunoreactivity to tyrosine hydroxylase (TH), that exist in CBs of female $SDHD^{+/-}$ (44.3 ± 1.3%; $n = 4$) compared with $SDHD^{+/+}$ (37.8 ± 1.5%; $n = 3$) animals (Fig. 6). The subtle glomus cell hyperplasia and organ hypertrophy probably precede tumor transformation, although we so far have not observed CB tumors in $SDHD^{+/-}$ mice. In humans, loss of heterozygosity (LOH) of the wild-type allele is required for PGL to occur (3, 4). The absence of tumors in the $SDHD^{+/-}$ mice suggests that the induction of LOH in CB glomus cells depends on different factors in humans and rodents. However, since systematic occurrence of pathologies associated with complex II deficiency depends on age (23), the possibility that CB paragangliomas could appear in aged $SDHD^{+/-}$ mice cannot be ruled out.

DISCUSSION

We report here a mammalian genetic model of SDH deficiency. To our knowledge, this is the first knockout mouse for a component of the mitochondrial electron transport chain. We show that the complete lack of the SDHD subunit is lethal during embryonic development and that partial SDHD deficiency produces a ~50% generalized decrease of the mitochondrial complex II activity, as determined by enzymatic assay of succinate dehydrogenase activity in isolated mitochondria. It has been shown that mutation of the SDHC homolog in *Caenorhabditis elegans* results in >80% reduction of complex II activity (10). The null *C. elegans* mutant is to some extent viable due to a small remaining SDH activity. Interestingly, this is not the case for the *SDHD* knockout mouse model, where the complete absence of the gene prevents embryo development. Lethality occurs in the early stages of organogenesis, most likely between 6.5 and 7.5 dpc, possibly due to the high energetic demands of embryos and/or to the general metabolic modifications resulting from the accumulation of succinate. We have not observed in the heterozygous $SDHD^{+/-}$ mouse a gene dosage compensation by overexpression of the wild-type allele. It is noteworthy that this functional deficit was similar in

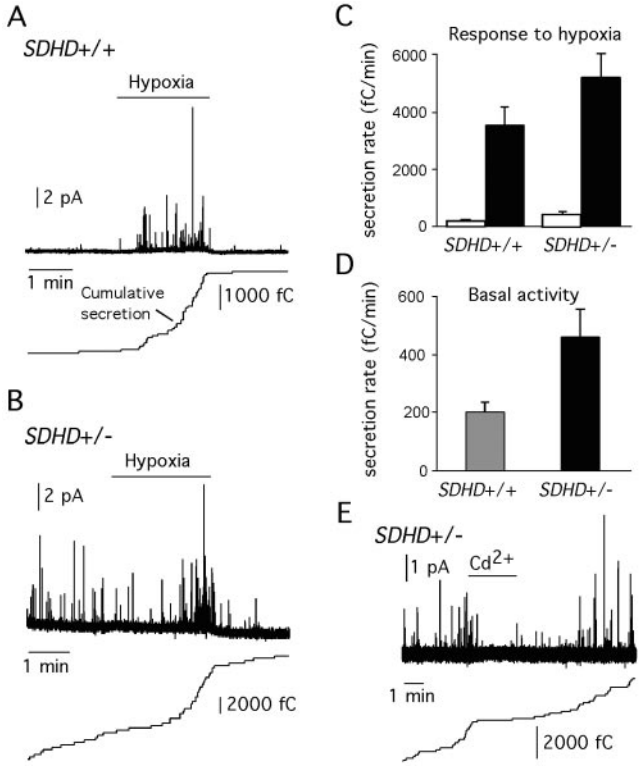

FIG. 4. Secretory activity and responsiveness to hypoxia of CB cells. (A and B) Secretory response to hypoxia of CB cells of $SDHD^{+/+}$ (A) and $SDHD^{+/-}$ (B) mice. Spike-like quantal events correspond to catecholamine release from individual vesicles. Cumulative secretion (in femtocoulombs) for each experiment is shown. (C) Quantification of the secretory response to low O_2 tension (in femtocoulombs/last minute of hypoxia) in SDHD-deficient (5,105 ± 810 fC/min [mean ± standard error]; $n = 16$) and wild-type (3,539 ± 603 fC/min; $n = 18$) mice ($P = 0.12$ by analysis of variance). (D) Quantification of the spontaneous secretory activity in CB slices from $SDHD^{+/+}$ (462 ± 94 fC/min [mean ± standard error]; $n = 16$) and wild-type (198 ± 35 fC/min; $n = 18$) mice ($P = 0.01$ by the Kruskal-Wallis test). (E) Spontaneous secretory activity in a $SDHD^{+/-}$ CB cells and reversible blockade by application of 0.3 mM extracellular cadmium.

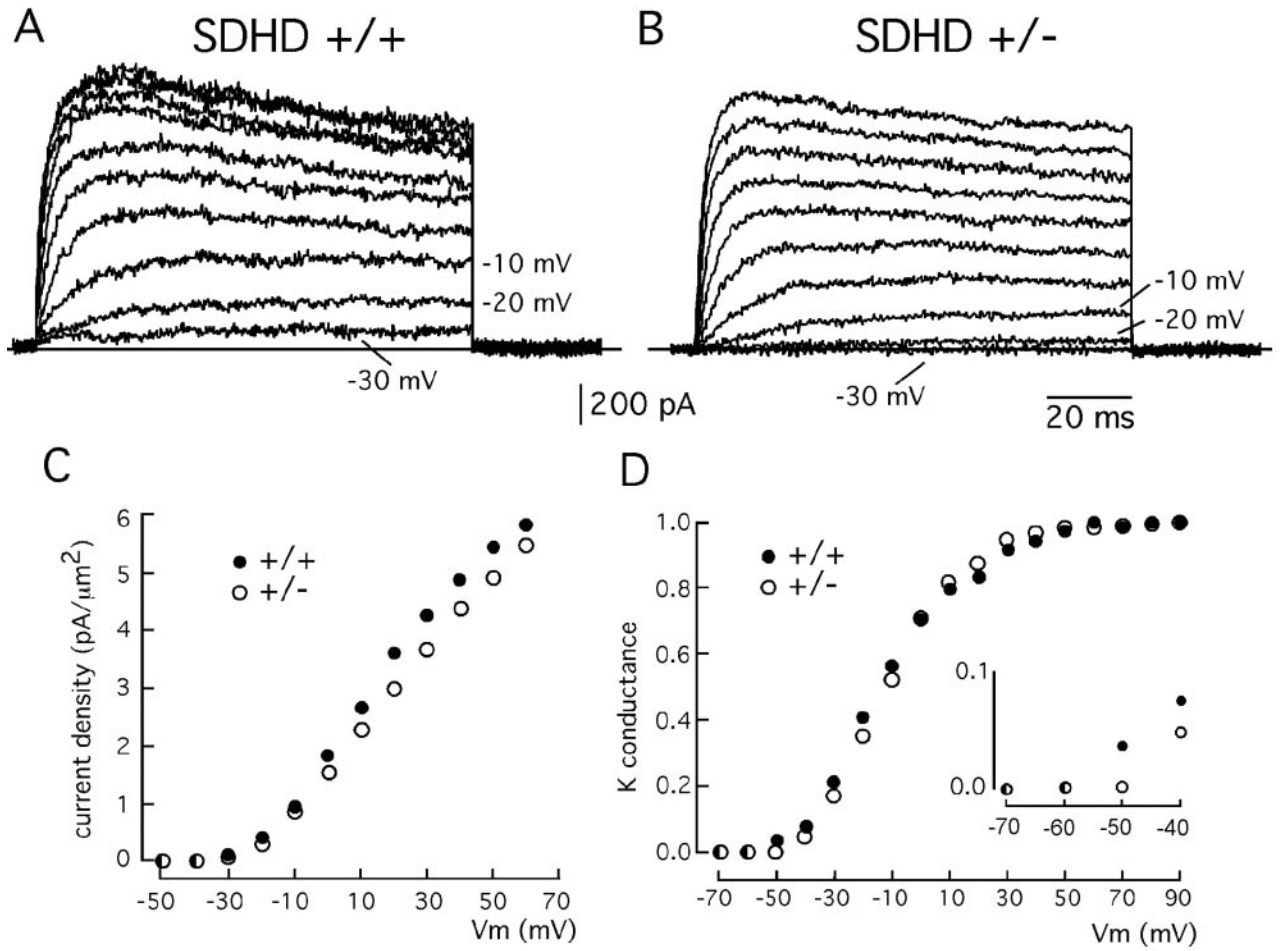

FIG. 5. Macroscopic K^+ currents in patch-clamped dispersed glomus cells of wild-type and partially SDHD-deficient mice. (A and B) Families of representative outward K^+ currents in $SDHD^{+/+}$ and $SDHD^{+/-}$ glomus cells recorded during 100-ms depolarizing pulses reaching membrane potentials between −30 and +60 mV in steps of 10 mV. (C) K^+ current density (ordinate)-versus-voltage (abscissa) relationship in wild-type and $SDHD^{+/-}$ glomus cells. Each point is the average from at least eight different experiments. (D) Normalized K^+ conductance (ordinate)-versus-voltage (abscissa) relationship in wild-type and $SDHD^{+/-}$ glomus cells. Each point is the average from at least three different experiments. Data points were fitted by an equation of the form $G = 1/[1 + \exp(V_{1/2} - V_m)/k]$. The half activation ($V_{1/2}$) (−11.7 and −10.6 mV for $SDHD^{+/+}$ and $SDHD^{+/-}$, respectively) and the slope factor (k) (14.6 and 12.6 mV for $SDHD^{+/+}$ and $SDHD^{+/-}$, respectively) were similar for the two curves. However, the activation threshold was clearly higher in $SDHD^{+/-}$ glomus cells (inset in panel D). In panels C and D, error bars are omitted.

tissues with relatively high (heart or kidney) and low (liver and brain) levels of SDH activity, pointing to a generalized deficit of succinate dehydrogenase activity. Strikingly, this SDH deficiency did not produce any gross morphological alteration or changes in body weight in $SDHD^{+/-}$ animals. Whether the existing mitochondrial SDH activity is sufficient to meet the metabolic demands of the tissues in vivo or whether there is a systemic compensation of SDH activity that is not detectable in

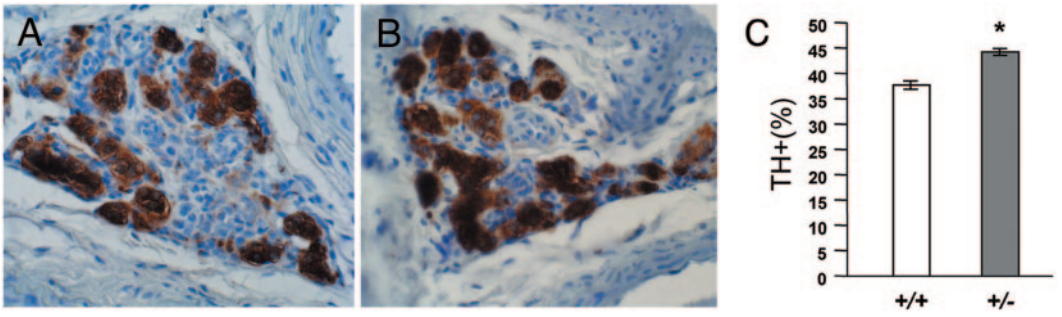

FIG. 6. (A and B) Immunohistochemistry of $SDHD^{+/+}$ (A) and $SDHD^{+/-}$ (B) carotid bodies. Tissues were incubated with an antibody to TH after which they were counterstained with hematoxylin for counting of nuclei. Note the cluster organization of glomus cells. (C) Percentage of TH-positive cells in the CBs of female mice ($n = 3$ for $SDHD^{+/+}$; $n = 6$ for $SDHD^{+/-}$). The asterisk indicates statistical significance ($P < 0.05$).

the mitochondrial assay are questions that remain to be investigated.

Detailed analysis of CB function in *SDHD*$^{+/-}$ animals has allowed us to detect a persistent CB overstimulation that resembles the Ca^{2+}-dependent CB activation induced by pharmacological inhibition of the mitochondrial electron transport chain (18). Electrophysiological studies on glomus cells suggest that a subtle, but measurable, decrease in the density and activation threshold of Ca^{2+}-dependent K^+ channels in *SDHD*$^{+/-}$ individuals could account for the persistent secretory activity of CB cells. However, future experiments should address how defects in SDHD activity lead to K^+ channel dysfunction. In this respect, it is tempting to speculate that formation of reactive oxygen species at complex II might play a role, as has been proposed for hypoxic pulmonary vasculature (19), but this has yet to be shown in *SDHD*$^{+/-}$ mice.

The functional changes observed in *SDHD*$^{+/-}$ CB cells are not accompanied by major histological modifications. We have detected an increase in the *SDHD*$^{+/-}$ glomus cell membrane surface, which could reveal some degree of cell hypertrophy. Immunohistochemical studies have also shown a small but significant increase in the percentage of TH-positive cells in the CBs of female *SDHD*$^{+/-}$ mice with respect to wild-type animals. Whether this is due to an increase in the expression of TH or to proliferation of glomus cells is unknown. Nevertheless, increases either in cell volume and number or in TH expression are hallmarks of hypoxia-induced CB hypertrophy (25). The constitutive CB overstimulation, which implies a constant Ca^{2+} influx and the activation of Ca^{2+}-dependent biochemical events in CB cells, is probably one of the mechanisms that induce first cellular hypertrophy and hyperplasia and subsequently tumor transformation in *SDHD*$^{+/-}$ patients. The fact that hereditary PGL shares histological characteristics with CBs exposed to chronic hypoxia (3, 4) and the higher frequency of *SDHD* mutant alleles in populations living at low altitudes (2) have led to the suggestion that SDHD participates in CB responses to lowering O_2 tension. We have shown that CB responsiveness to hypoxia was not impaired in the mutant *SDHD*$^{+/-}$ mice despite a 50% generalized decrease in SDH activity, and persistent CB overstimulation was observed. Although it has not yet been possible to test the responsiveness to hypoxia of *SDHD*$^{-/-}$ glomus cells, the data available so far suggest that SDHD is not directly responsible for CB acute O_2 sensing.

Tumor formation in hereditary CB PGL appears to require the LOH of the *SDHD* wild-type allele. To date, we have not observed an increased susceptibility to tumorigenesis in our mouse model. Thus, it is likely that the biological determinants making the human *SDHD* region a hot spot for LOH do not exist in mouse. On the other hand, the rate of PGL tumor onset, like that of most of the pathologies associated with mitochondrial complex II deficiencies, depends on age (1, 22, 23). Since the average age of the mice in our colony does not reach 1 year, we cannot exclude the possibility that tumors will appear in aged mice. As in the CB, somatic SDHD deficiency could also produce constitutive subclinical alterations in other organs, especially in those containing paraneural tissues, where the decrease of complex II activity precedes the appearance of diseases (8, 13, 17). The SDHD knockout mouse model could help to provide prognostic insights for individuals carrying mutations. In addition, it could be a valuable tool for the study of the pathophysiological mechanisms that induce LOH-dependent tumorigenesis and other pathologies associated with SDHD deficiency in humans.

ACKNOWLEDGMENTS

We thank J. H. Hoeijmakers and R. Fernández-Chacón for the supply of mouse ES lines and J. A. Enríquez for technical advice.

J. López-Barneo received the Ayuda a la Investigación 2000 of the Juan March Foundation. Research was also supported by The Lilly Foundation and by grants from the Spanish Ministries of Health and of Science and Technology.

REFERENCES

1. **Ackrell, B. A.** 2002. Cytopathies involving mitochondrial complex II. Mol. Aspects Med. **23:**369–384.
2. **Astrom, K., J. E. Cohen, J. E. Willett-Brozick, C. E. Aston, and B. E. Baysal.** 2003. Altitude is a phenotypic modifier in hereditary paraganglioma type 1: evidence for an oxygen-sensing defect. Hum. Genet. **113:**228–237.
3. **Baysal, B. E., R. E. Ferrell, J. E. Willett-Brozick, E. C. Lawrence, D. Myssiorek, A. Bosch, A. van der Mey, P. E. Taschner, W. S. Rubinstein, E. N. Myers, C. W. Richard III, C. J. Cornelisse, P. Devilee, and B. Devlin.** 2000. Mutations in *SDHD*, a mitochondrial complex II gene in hereditary paraganglioma. Science **287:**848–851.
4. **Baysal, B. E.** 2003. On the association of succinate dehydrogenase mutations with hereditary paraganglioma. Trends Endocrinol. Metab. **14:**453–459.
5. **Birch-Machin, M. A., and D. M. Turnbull.** 2001. Assaying mitochondrial respiratory complex activity in mitochondria isolated from human cells and tissues. Methods Cell Biol. **65:**97–117.
6. **Fernandez-Vizarra, E., M. J. Lopez-Perez, and J. A. Enriquez.** 2002. Isolation of biogenetically competent mitochondria from mammalian tissues and cultured cells. Methods **26:**292–297.
7. **Gimenez-Roqueplo, A. P., J. Favier, P. Rustin, J. J. Mourad, P. F. Plouin, P. Corvol, A. Rotig, and X. Jeunemaitre.** 2001. The R22X mutation of the *SDHD* gene in hereditary paraganglioma abolishes the enzymatic activity of complex II in the mitochondrial respiratory chain and activates the hypoxia pathway. Am. J. Hum. Genet. **69:**1186–1197.
8. **Habano, W., T. Sugai, S. Nakamura, N. Uesugi, T. Higuchi, M. Terashima, and S. Horiuchi.** 2003. Reduced expression and loss of heterozygosity of the *SDHD* gene in colorectal and gastric cancer. Oncol. Rep. **10:**1375–1380.
9. **Hederstedt, L.** 2003. Complex II is complex too. Science **299:**671–672.
10. **Ishii, N., M. Fujii, P. S. Hartman, M. Tsuda, K. Yasuda, N. Senoo-Matsuda, S. Yanase, D. Ayusawa, and K. Suzuki.** 1998. A mutation in succinate dehydrogenase cytochrome b causes oxidative stress and ageing in nematodes. Nature **394:**694–697.
11. **Lahiri, S., N. R. Prabhakar, and R. E. Forster.** 2000. Oxygen sensing. Molecule to man. Kluwer Academic/Plenum Publishers, New York, N.Y.
12. **Lancaster, C. R. D.** 2002. Succinate:quinone oxidoreductases: an overview. Biochim. Biophys. Acta **1553:**1–6.
13. **Lima, J., J. Teixeira-Gomes, P. Soares, V. Maximo, M. Honavar, D. Williams, and M. Sobrinho-Simoes.** 2003. Germline succinate dehydrogenase subunit D mutation segregating with familial non-RET C cell hyperplasia. J. Clin. Endrocrinol. Metab. **88:**4932–4937.
14. **López-Barneo, J., R. Pardal, and P. Ortega-Sáenz.** 2001. Cellular mechanism of oxygen sensing. Annu. Rev. Physiol. **63:**259–287.
15. **López-Barneo, J.** 2003. Oxygen and glucose sensing by carotid body glomus cells. Curr. Opin. Neurobiol. **13:**493–499.
16. **López-López, J. R., C. González, and M. Pérez-García.** 1997. Properties of ionic currents from isolated adult rat carotid body chemoreceptor cells: effect of hypoxia. J. Physiol. **499:**429–441.
17. **Maier, W., N. Marangos, and R. Laszig.** 1999. Paraganglioma as a systemic syndrome: pitfalls and strategies. J. Laryngol. Otol. **113:**978–982.
18. **Ortega-Sáenz, P., R. Pardal, M. García-Fernández, and J. López-Barneo.** 2003. Rotenone selectively occludes sensitivity to hypoxia in rat carotid body glomus cells. J. Physiol. **548:**789–800.
19. **Paddenberg, R., A. Goldenberg, P. Faulhammer, R. C. Braun-Dullaeus, and W. Kummer.** 2003. Mitochondrial complex II is essential for hypoxia-induced ROS generation and vasoconstriction in the pulmonary vasculature. Adv. Exp. Med. Biol. **536:**163–169.
20. **Pardal, R., U. Luwewig, J. García-Hirschfeld, and J. López-Barneo.** 2000. Secretory responses of intact glomus cells in thin slices of rat carotid body to hypoxia and tetraethylammonium. Proc. Natl. Acad. Sci. USA **97:**2361–2366.
21. **Peers, C.** 1990. Hypoxic suppression of K^+ currents in type I carotid body cells: selective effect on the Ca^{2+}-activated K^+ current. Neurosci. Lett. **119:**253–256.
22. **Rustin, P., A. Munnich, and A. Rötig.** 2002. Succinate dehydrogenase and human diseases: new insights into a well-known enzyme. Eur. J. Hum. Genet. **10:**289–291.
23. **Rustin, P., and A. Rötig.** 2002. Inborn errors of complex II. Unusual human mitochondrial diseases. Biochim. Biophys. Acta **1553:**117–122.

24. **Ureña, J., R. Fernández-Chacón, A. R. Benot, G. Alvarez de Toledo, and J. López-Barneo.** 1994. Hypoxia induces voltage-dependent Ca^{2+} entry and quantal dopamine secretion in carotid body glomus cells. Proc. Natl. Acad. Sci. USA **91:**10208–10211.
25. **Wang, Z. Y., and G. E. Bisgard.** 2002. Chronic hypoxia-induced morphological and neurochemical changes in the carotid body. Microsc. Res. Technol. **59:**168–177.
26. **Wyatt, C. N., and C. Peers.** 1995. Ca^{2+}-activated K^+ channels in isolated type I cells of the neonatal rat carotid body. J. Physiol. **483:**559–565.
27. **Yankovskaya, V., R. Horsefield, S. Tornroth, C. Luna-Chavez, H. Miyoshi, C. Leger, B. Byrne, G. Cecchini, and S. Iwata.** 2003. Architecture of succinate dehydrogenase and reactive oxygen species generation. Science **299:**700–704.